Nanometer-size P/K-rich silica glass (former melt) inclusions in microdiamond from the gneisses of Kokchetav and Erzgebirge massifs: Diversified characteristics of the formation media of metamorphic microdiamond in UHP rocks due to host-rock buffering

Shyh-Lung Hwang [a],*, Hao-Tsu Chu [b], Tzen-Fu Yui [c], Pouyan Shen [d], Hans-Peter Schertl [e], Juhn G. Liou [f], Nikolai V. Sobolev [g]

[a] Department of Materials Science and Engineering, National Dong Hwa University, Hualien, Taiwan, ROC
[b] Central Geological Survey, P.O. Box 968, Taipei, Taiwan, ROC
[c] Institute of Earth Sciences, Academia Sinica, Taipei, Taiwan, ROC
[d] Institute of Materials Science and Engineering, National Sun Yat-sen University, Kaohsiung, Taiwan, ROC
[e] Institut für Geologie, Mineralogie und Geophysik, Ruhr-Universitat Böchum, 44780 Bochum, Germany
[f] Department of Geological and Environmental Sciences, Stanford University, Stanford, CA 94305, USA
[g] Institute of Mineralogy and Petrography, Siberian Branch of Russian Academy of Sciences, 630090 Novosibirsk, Russia

Abstract

Nanometer-size P/K-rich silica glass (former melt) inclusions were identified within metamorphic microdiamonds from garnets of ultrahigh-pressure (UHP) gneisses of the Kokchetav and the Erzgebirge massifs by analytical electron microscopy (AEM). The chemical characteristics of these inclusions within microdiamonds are surprisingly similar among various gneissic rocks from both Kokchetav and Erzgebirge, but are significantly different from the Si-poor ultrapotassic fluid inclusions within microdiamonds from garnets of the Kokchetav UHP marble. These contrasting findings not only provide constraints on the characteristics/ compositions of the formation media of metamorphic microdiamonds, but also imply that the formation media must have been buffered by the hosting rocks, resulting in the observed diversities as reported here. In addition, depending on the rock types and thus on the nature of the formation media from which metamorphic microdiamonds were formed, the respective characteristic morphologies of the microdiamonds differ. The P/K-rich silica melt tends to form octahedral or cubo-octahedral microdiamonds within garnet in gneissic rocks, whereas the Si-poor ultrapotassic fluid tends to form spheroids/cuboid microdiamonds with rugged surfaces within garnet in marble. Consequently, the buffered media in hosting rocks played a decisive role in determining the different morphologies and growth rates/mechanisms of metamorphic microdiamonds in general.
© 2005 Elsevier B.V. All rights reserved.

Keywords: analytical electron microscopy (AEM); diamond; microdiamond; inclusion; fluid; glass; Kokchetav; Erzgebirge; ultrahigh-pressure metamorphism

---

* Corresponding author.
  E-mail address: slhwang@mail.ndhu.edu.tw (S.-L. Hwang).

1. Introduction

The finding of metamorphic microdiamonds as mineral inclusions in rocks of crustal composition in collision zones provides a piece of direct evidence that continental rocks could be subducted to mantle depths within the diamond stability field. The occurrence of such metamorphic microdiamonds was well characterized in situ in the Kokchetav massif of Kazakhstan [1], the Saxonian Erzgebirge of Germany [2] and the North Qinling zone of China [3]. The genesis of these metamorphic microdiamonds has been an intriguing issue, not only for understanding the formation mechanisms of these metamorphic diamonds but also for comparative genetic studies with kimberlitic mantle diamonds.

Since their discovery about 15 years ago [1], metamorphic microdiamonds have been considered to have undergone either transformation in solid state from graphite [4] or precipitation through a fluid/melt medium [5–8]. Although at high pressures a distinction between hydrous fluids and silicate melts might be difficult because the system could be in a supercritical state (ranging from low-density supercritical vapors to denser volatile-rich melts) [9], Hwang et al. [6] provided the first evidence on possible microdiamond genesis from a silicate melt. They showed that the microdiamonds from an Erzgebirge gneiss sample were constantly associated with mica(s), quartz, apatite, sulfides, as well as an amorphous SiO_2-rich material presumably formed from a melt during cooling, constituting multiple-phase inclusion pockets in garnets. This amorphous SiO_2-rich material with rounded surface showed characteristic diffused diffraction ring typical of silica glasses in electron diffraction experiments [6]. On the other hand, the FTIR characterization of water and carbonate inclusions in Kokchetav microdiamonds of a garnet–clinopyroxene rock was employed as the first convincing proof for a possible genesis of microdiamonds from a carbonate-rich COH fluid [5]. This was generalized to either a supercritical COH + silicate fluid by the observation of diamond-bearing polyphase inclusions in garnets from Erzgebirge gneisses [7], or a supercritical COH-rich multiple component fluid after the discovery of nanometric solid inclusions of oxides, carbonates and silicates in microdiamonds from Kokchetav gneisses [8]. Hwang et al. [10] further documented direct visual images of nanometer-size highly potassic COH fluid inclusions in microdiamonds from the Kokchetav dolomite marble by AEM. These fluid inclusions unambiguously illustrat-ed that the microdiamonds in the Kokchetav dolomite marble were precipitated from a salty fluid phase.

The ultrapotassic fluid phase within microdiamonds from marble is distinctly low in SiO_2 [10], and appears to be very different in chemical characteristics from the silicate melt phase postulated for the genesis of microdiamonds in Erzgebirge gneisses [6], although the true composition of such a silicate melt phase remains to be studied. Detailed AEM work on the identification/characterization of nanometer-size syngenetic P/K-rich silica glass (former melt) inclusions within microdiamonds from garnet-bearing gneissic rocks from the Kokchetav and the Erzgebirge UHP terranes were performed and reported here. This work was conducted in order to obtain a direct proof of the presence of silicate melts in UHP gneisses during microdiamond formation, to better constrain their chemical characteristics, and also to compare their compositions among different diamondiferous gneissic rocks from two major microdiamond-bearing UHP terranes. These observations, including ultrapotassic fluid inclusions in marble [10] and P/K-rich silica glass inclusions in gneisses, yield indisputable evidence that, in addition to the process of solid-state transformation from graphite [4], most metamorphic microdiamonds must have been formed from fluids or melts with distinct compositions. Using the new data presented here and the available ones given by Hwang et al. [10], we have managed to establish some interesting correlations between diamond morphology, formation medium characteristics and host rock types.

2. Sample description and methods

Three garnet-bearing gneissic samples from the Kokchetav massif of Kazakhstan (KD302, KD304, KD307) and one from the Saxonian Erzgebirge of Germany (25966) were selected for the present study. One gneiss (M1), two garnet–quartz–clinopyroxene rocks (K12A and KD301) and one dolomite marble (KD81), which were previously studied by Hwang et al. [6,10,11], were also included in the present study for re-examination.

The geologic background of the Kokchetav massif and the Saxonian Erzgebirge have recently been reviewed by Shatsky and Sobolev [12] and by Massonne and O'Brien [13], respectively; both emphasize the presence of microdiamond inclusions in minerals such as garnet, clinopyroxene, kyanite, etc., in crustal gneissic, carbonate, and garnet–clinopyroxene rocks subjected to metamorphic conditions $T > 950$ °C and $P > 40$ kbar.

All samples from the Kokchetav massif were collected from the gallery of a mine [14] in Kumdy-Kol, Kazakhstan, containing diamond-bearing UHP metamorphic rocks. Samples KD302, KD304 and KD307 are garnet–biotite gneisses, which consist mainly of coarse-grained garnet in a matrix of biotite–muscovite, quartz, plagioclase, chlorite, calcite, rutile–titanite, and graphite. Samples K12A and KD301 are garnet–quartz–clinopyroxene rocks with minor biotite, amphibole, chlorite, phengite, titanite, calcite, zircon, and opaques. Dolomite marble (sample KD81) is medium to coarse-grained and contains dolomite, garnet, diopside, phlogopite, and minor amounts of chlorite, titanite, graphite, and opaques [12]. Microdiamond inclusions are present in garnets of all these samples.

Sample 25966, as well as sample M1, are quartzofelspathic gneisses collected near the eastern shore of the Saidenbach reservoir about 1.5 km NE of the village of Forchheim in Erzgebirge, Germany. The gneiss samples are composed of relatively large garnet crystals in a matrix of quartz, phengite, biotite, kyanite, albitic plagioclase, K-feldspar, zircon, rutile, and graphite. Microdiamond inclusions are abundant in garnet crystals [2].

Thin sections showing garnet grains with diamond-bearing inclusion pockets under optical microscope were first clamped between two copper rings to ensure sample integrity, followed by argon-ion-beam milling (Gatan, PIS) to perforation (operation condition: 4.0 kV, 9° incident angle). A total of 37 AEM discs containing microdiamonds at the thinned edge of garnet grains were analyzed in the present study. These discs were prepared from the following samples: G1–G12 from sample KD302, G1–G9 from sample KD304, G1–G8 from sample KD307, and SE1–SE8 from sample 25966. Additional 13 newly prepared AEM discs from the samples of our previous studies (M1, K12A, KD301 and KD81) were also examined. The specimens were coated by carbon after ion thinning. Microstructure and compositions of minerals were studied using an AEM (JEOL JEM-3010 operated at 300 kV) equipped with an energy dispersive X-ray (EDX) spectrometer (Oxford EDS-6636) with an ultra-thin window and a Si(Li) detector, capable of detecting elements from boron to uranium. EDX spectra of inclusions were collected for 150–200 s. Absorption corrections were applied by assuming uniform distribution of oxides in the carbon matrix. Although this assumption may introduce 10–20% underestimation of light elements such as Na, errors for heavier elements are negligible [15]. For each analysis, a reference spectrum was also obtained from the proximate diamond matrix free of inclusions, which was then subtracted from the inclusion spectrum to remove the spurious X-rays, including Cu, Fe and Cr (supporting ring, sample stage), Ar (ion milling) and film counts (rock matrix), before performing semi-quantitative oxide fraction calculations [16]. In general, the statistical precision was about ±5–10% for the major elements Si, P and K, and ±20–30% for other minor elements.

3. Results

3.1. Garnet–biotite gneiss (KD302, KD304 and KD307) from Kokchetav

Optical microscopic (OM) observations showed micrometer-size diamond and graphite as independent or associated inclusions within garnet. Most microdiamonds are single crystals with sizes ranging between 3 and 20 μm. The average size varies around 6–10 μm. Some graphite inclusions in fact have a transparent diamond core as revealed by Ar ion-milling to remove the graphite shell. Associated phases include chlorite, pyrophyllite, Ti-bearing biotite, Ti-bearing phengite, calcite, dolomite and metal sulfide.

OM and AEM observations showed that microdiamond generally has cubo-octahedral habit bounded by {111} and {100} faces (Fig. 1a), although other irregular boundaries consisting of nanometer-size {111} growth steps were also observed. Tiny facetted inclusions, as small as 1–5 nm (generally <20–30 nm) in size, were found within microdiamonds (Fig. 2a). Whereas these nano-size inclusions are common in almost all microdiamonds in samples KD304 and KD307, microdiamonds from sample KD302 contain only a few of those inclusions. Typically, these tiny inclusions are facetted with {111} faces of diamond. Except for the pale black contrast due to the presence of elements heavier than carbon (to be addressed below) under AEM, these tiny inclusions are in all probability amorphous since they, either intact or mechanically opened by ion-milling, did not show any sign of diffraction contrast upon sample tilting (Fig. 2a). The amorphous nature of these inclusions was further confirmed by high-resolution images showing only the lattice-fringes from the overlying/underlying diamond matrix. It is possible that the size-effect (surface energy effect) hindered the crystallization processes in these nano-size inclusions during cooling. Spherical secondary fluid droplets, typically developed within fluid inclusions in microdiamonds from marble under
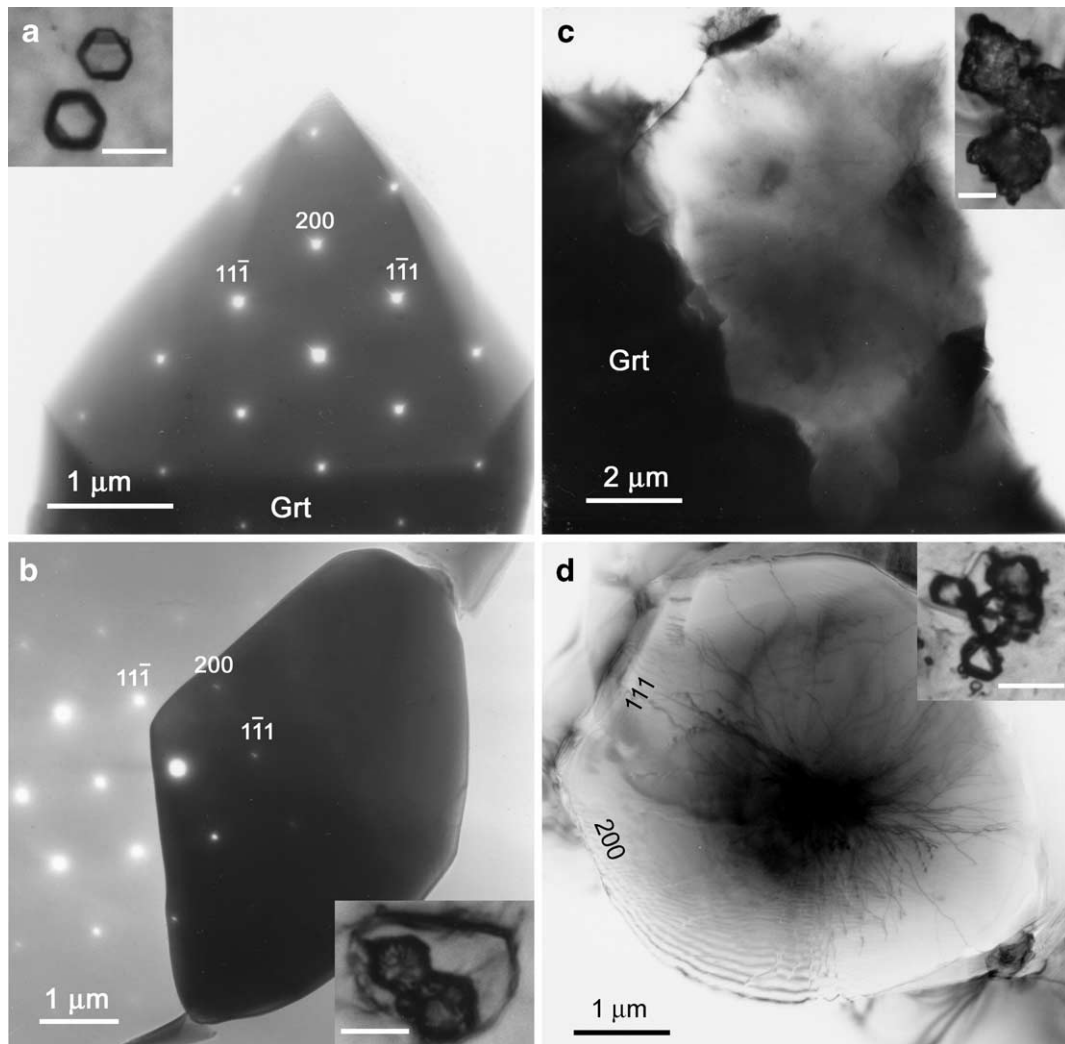
Fig. 1. AEM bright field images with insets of optical micrographs showing the growth forms of microdiamonds: (a) cubo-octahedral form ([011] zone axis as indicated by the superimposed electron diffraction pattern) in gneiss of Kokchetav, (b) cubo-octahedral form ([011] zone axis as indicated by the superimposed electron diffraction pattern) in gneiss of Saxonian Erzgebirge, (c) cuboid/spheroid form in marble of Kokchetav, and (d) cubo-octahedral form in garnet–quartz–clinopyroxene rock of Kokchetav. Radiating bundle of dislocations originating from the center of diamond crystals is also shown in (d). Scale bars in insets = 10 μm.

electron beam heating [10], were not observed in these inclusions.

Broad beam EDX analyses of inclusions showed high contents of Si, K, P and Cl (Fig. 3a) (Table 1). Compositional variations among inclusions are common. Despite the tiny size, the individual inclusion is also in many cases not uniform in composition, and variation from a Si-rich portion to a P- and K-rich portion in a single inclusion was frequently detected in EDX analyses using 5 nm spots (Fig. 4). It is important to note that mechanically opened inclusions typically are characterized by lower Cl/Si, P/Si and K/Si ratios than intact inclusions (Fig. 3b; see sample KD304-G8/ 22 in Table 1). This may indicate the presence of a volatile phase rich-in Cl, P and K, which escaped from the opened inclusions during sample preparation. The reported complex solid inclusion suite in microdiamonds from felsic gneiss of Kokchetav [8], including various oxides, rare carbonates and silicates, was not observed in all microdiamonds of the 29 AEM discs examined here.

The above observations are in many respects different from those of potassium-rich fluid inclusions (Table 2) in metamorphic microdiamond from Kokchetav marble reported by Hwang et al. [10]. Importantly, whereas the fluid inclusions in microdiamonds within
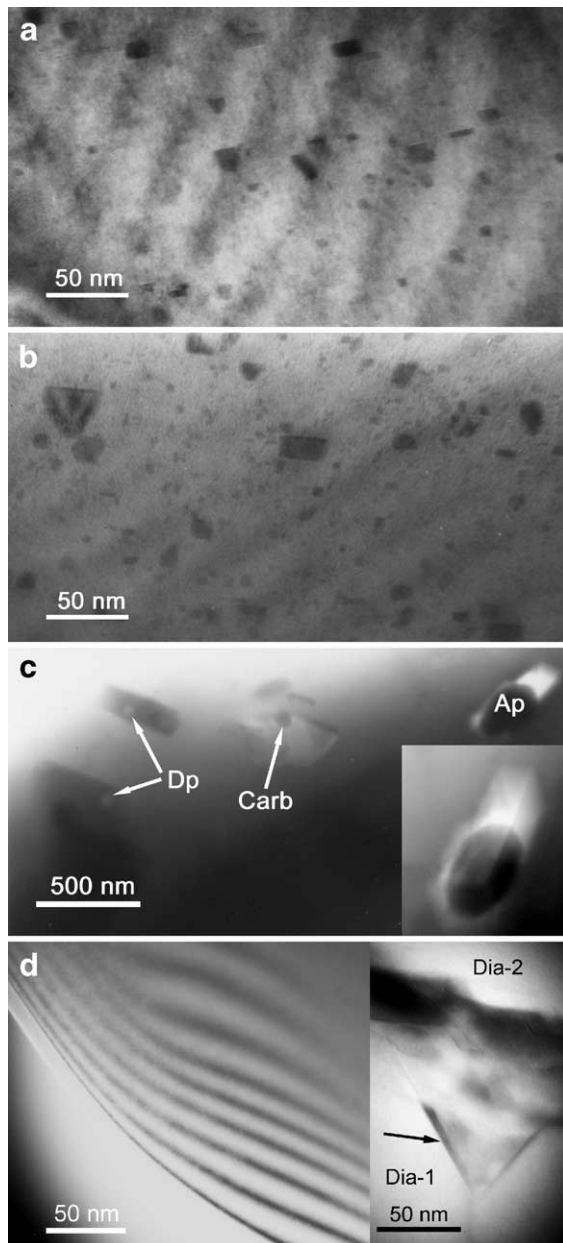
Fig. 2. AEM bright field images showing the faceted inclusions within metamorphic microdiamonds from (a) gneis of Kokchetav, (b) gneiss of Saxonian Erzgebirge, and (c) marble of Kokchetav. The secondary fluid droplets (Dp) formed in intact inclusions upon electron beam heating, as well as (K,Ca)-carbonate (Carb) and apatite (Ap) in opened inclusions are marked in (c). The large free volume in the opened pocket containing apatite in (c) could be better seen in the inset with higher magnification. The microdiamond without inclusions from garnet–quartz–clinopyroxene rocks of Kokchetav is shown in (d). The inset of (d) shows a typical faceted intergranular pocket (arrowed) within diamond aggregates in garnet from garnet–quartz–clinopyroxene rocks.

garnet of the Kokchetav marble from the previous studies [10] are abundant, much larger in size (i.e. <500 nm), and showed Bragg diffraction contrast from the solid precipitates upon sample tilting during AEM studies, the glass inclusions in microdiamonds within garnet from the gneissic rocks are less abundant, smaller in size (i.e., <30 nm), and did not show any Bragg diffraction contrast upon sample tilting. The lack of Bragg diffraction contrast yet the rigid condition for both intact and mechanically opened inclusions strongly suggests that the inclusions in microdiamonds from garnet–biotite gneisses are most likely glass (+exsolved vapor/fluid) (i.e. former melt) inclusions, but not fluid inclusions. The observed spectral differences between the intact and opened inclusions (Fig. 3), demonstrated by the lack of Cl in opened pockets and by the variations in the Si/K and Si/P atomic ratios from <5 and <7 in intact pockets to ~11 and ~8 in opened pockets (see sample KD 304 in Table 1), indicate a preferential partitioning of elements (relative to Si) into the exsolved vapor/fluid phase in vapor/fluid-melt systems during cooling (see also [17,18]).

3.2. Quartzofeldspathic gneiss (25966 and M1) from Erzgebirge

Microdiamonds with sizes ranging between 3 and 18 μm (~9 μm in average) are usually associated with quartz, apatite, micas and metal sulfides/arsenides (ZnS and (Ni,Co)As) as multiphase inclusions in garnet as described by Hwang et al. [6]. Although more or less rounded in multiple phase pockets in OM micrographs (Fig. 1b), AEM did reveal that these microdiamonds beautifully preserve octahedral/cubo-octahedral morphology when in contact with garnet matrix (Fig. 1b), although irregular boundaries with nanometer-scale {111} terrace and rough ledge of diamond in contact with mica or quartz were also observed. Many faceted pockets less than 20 nm in size were also identified in these microdiamonds (Fig. 2b); these pockets were previously mistaken as nitrogen platelets [6]. However, careful EDX analyses in the present study revealed that these pockets are in fact P/K-rich silica glass inclusions compositionally similar to the glass inclusions in microdiamonds within garnet from the garnet–biotite gneisses of Kokchetav mentioned above, except for lower Cl content (Fig. 3c; Table 1). These glass inclusions in microdiamonds from Erzgebirge, like those from Kokchetav, show spatial compositional variations within one individual pocket, and have high Si, low
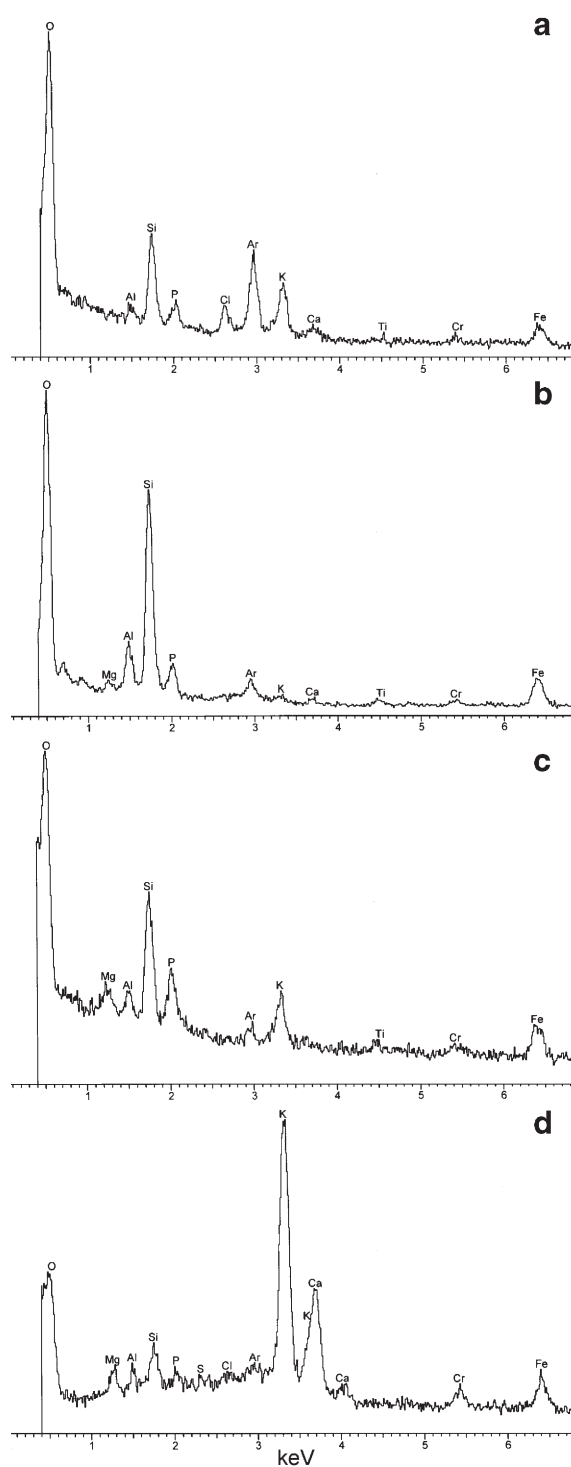
Fig. 3. Representative EDX spectra from (a) intact and (b) opened glass inclusions in gneiss of Kokchetav, (c) intact glass inclusions in gneiss of Saxonian Erzgebirge, and (d) intact fluid inclusions in marble of Kokchetav. The Cr counts and most of the Fe counts in the spectra were originated from AEM sample stage. The abscissa is X-ray energy in the unit of keV and the ordinate is X-ray intensity.

P and K contents in opened ones (see sample 25966-SE6-17 in Table 1). Trace opened inclusions with only Si or Si+Al contents were also observed. Inclusions as large as 200 nm in size, as well as empty pockets which had been cited as evidence for a former COH fluid [19], were not observed in the present samples.

3.3. Dolomite marble (KD81) from Kokchetav

To provide a contrasting comparison, in terms of size, abundance and distribution, between fluid inclusions within microdiamonds from marble and glass inclusions within microdiamonds from gneissic rocks, as well as to demonstrate the morphological/microstructural features of microdiamonds from marble under AEM, additional AEM micrographs and EDX spectrum taken from 3 newly prepared AEM discs of sample KD81 in the previous study [10] are also included here.

According to OM and AEM observations, microdiamond inclusions (up to 35 μm in diameter) in garnet are usually cuboid or spheroid in shape with very rugged surfaces (Fig. 1c), and occasionally are associated with phlogopite. Dark field images indicated that most microdiamonds are single crystals yet with abundant subgrain boundaries and dislocations, probably resulting from the columnar growth mechanism responsible for the formation of cuboid/spheroid shape [20]. There are abundant nano-size ultrapotassic fluid inclusions (<500 nm) in these microdiamonds (Fig. 2c). These highly potassic fluid inclusions are extremely low in SiO_2 according to AEM-EDX (Fig. 3d). Spherical secondary fluid droplets with brighter contrast were readily formed in such pockets within ∼1 min of exposure to focused electron beam and were able to migrate in the inclusion pockets under the influence of electron beam heating (arrowed in Fig. 2c). Such an observation was attributed to the formation of two immiscible phases, a carbonatitic fluid and a hydrous fluid, upon electron-beam heating and possible decompression in Hwang et al. [10]. The fluid nature of these inclusions was further supported in the present study by the observations of large free volume, some greater than 50 vol.%, in the opened (and then drained) pockets (see the opened pocket with apatite, inset in Fig. 2c), as well as by the dramatic compositional differences between the intact and the opened (and then drained) pockets as presented in Hwang et al. [10]. Solid precipitates including apatite, carbonate, sulfide/sulfate, chloride, silicate and oxide were also frequently observed in the inclusions (Fig. 2c).

Table 1
Semi-quantitative chemical compositions, on a volatile-free basis, of glass inclusions (wt.%) in metamorphic microdiamonds from gneissic rocks

Sample no.	KD302-G2-17	KD304-G1-1	KD304-G2-1	KD304-G8-24	KD304-G8-45	KD304-G8-49	KD304-G9-16	KD304-G9-21	KD304-G9-23	KD304-G8-22[a]	KD307-G2a-76
SiO_2	47	39	47	55	59	45	52	50	64	70	62
TiO_2	trace	trace	trace	trace	bdl [b]	trace	bdl	bdl	bdl	bdl	bdl
Al_2O_3	trace	15	8	2	2	2	bdl	9	12	8	6
FeO	1	bdl	1	trace	3	trace	bdl	trace	bdl	4	2
MgO	2	1	1	bdl	2	6	bdl	4	bdl	1	3
CaO	2	bdl	bdl	bdl	bdl	4	bdl	bdl	bdl	1	2
Na_2O	bdl	bdl	bdl	bdl	bdl	bdl	bdl	bdl	bdl	bdl	bdl
K_2O	21	13	12	18	16	24	18	19	11	5	13
P_2O_5	19	30	21	23	13	12	22	11	10	11	6
S	trace	trace	3	bdl	trace	trace	trace	bdl	trace	bdl	trace
Cl	8	2	7	2	5	7	8	7	3	bdl	6
Si/K[c]	1.75	2.28	3.00	2.41	2.97	1.50	2.24	2.04	4.59	11.14	3.70
Si/P[c]	2.95	1.50	2.62	2.91	5.49	4.38	2.71	5.70	7.28	7.68	12.47

Sample no.	KD307-G8-7	M1-G3-16	25966-SE2-13	25966-SE2-16	25966-SE5-16	25966-SE6-2	25966-SE6-22	25966-SE6-28	25966-SE6-17[a]	KD81-G24/50[d]	KD301-G24/50[d]
SiO_2	43	67	51	56	54	61	43	59	85	8	25
TiO_2	bdl	trace	1	trace	trace	1	trace	trace	trace	bdl	trace
Al_2O_3	12	9	3	10	bdl	3	bdl	9	10	1	1
FeO	bdl	1	1	3	bdl	1	trace	1	trace	3	6
MgO	1	2	bdl	bdl	bdl	2	9	2	bdl	6	7
CaO	3	trace	bdl	1	10	2	bdl	bdl	bdl	19	21
Na_2O	bdl	bdl	bdl	bdl	bdl	bdl	bdl	bdl	bdl	bdl	bdl
K_2O	21	5	13	9	18	18	18	8	3	57	32
P_2O_5	17	16	31	20	17	11	31	21	2	3	5
S	bdl	bdl	bdl	trace	trace	trace	trace	trace	bdl	1	1
Cl	3	bdl	trace	1	1	1	bdl	bdl	bdl	2	2
Si/K[c]	1.64	10.44	2.98	4.97	2.32	2.72	1.90	5.65	24.25	0.11	0.61
Si/P[c]	3.09	5.08	1.97	3.33	3.79	6.85	1.65	3.40	41.96	2.69	5.96

[a] Opened pocket.

[b] bdl: below detection limit.

[c] Atomic ratio.

[d] Representative chemical composition of fluid inclusion in diamond from dolomite marble (KD81) and garnet–quartz–clinopyroxene rock (KD301), respectively. Data were taken from Hwang et al. [10] for comparison.

3.4. Garnet–quartz–clinopyroxene rock (K12A and KD301) from Kokchetav

It has always been difficult to observe/characterize the nano-size glass inclusions within microdiamonds despite the use of AEM techniques. This is mainly due to the tiny size, the low atomic contrast and the lack of diffraction contrast of those inclusions, which could readily cause the glass inclusions to be overlooked in AEM studies. To further verify the results in Hwang et al. [10,11] regarding the absence of intragranular inclusions within microdiamonds from garnet–quartz–clinopyroxene rocks of the Kokchetav massif, and also to show the morphological/microstructural features of microdiamonds in garnet–quartz–clinopyroxene rocks observed by AEM, additional 8 AEM disks from samples KD301 [10] and K12A [11] were newly prepared, examined, and reported here.

Metamorphic cubo-octahedral microdiamonds of 3–10 µm in size (∼6 µm on average), with well-developed {111} and {100} faces, occur in garnets from garnet–quartz–clinopyroxene rocks (Fig. 1d). Polycrystalline aggregates composed of octahedral microdiamonds are also common. Radiating bundles of dislocations originating from the center of diamond crystals and connected to the surface trigons were also observed, indicating a prevailing fluid/melt layer growth mechanism (Fig. 1d). The observed cubo-octahedral/octahedral morphology and dislocation microstructure are unlikely due to solid-state transformation from graphite. It is important to note that, in contrast to the microdiamonds within garnets from gneisses and marbles, no intragranular inclusions were observed by AEM in microdiamonds from the garnet–quartz–clinopyroxene rocks (Fig. 2d). However, several faceted intergranular pockets within a microdiamond aggregate
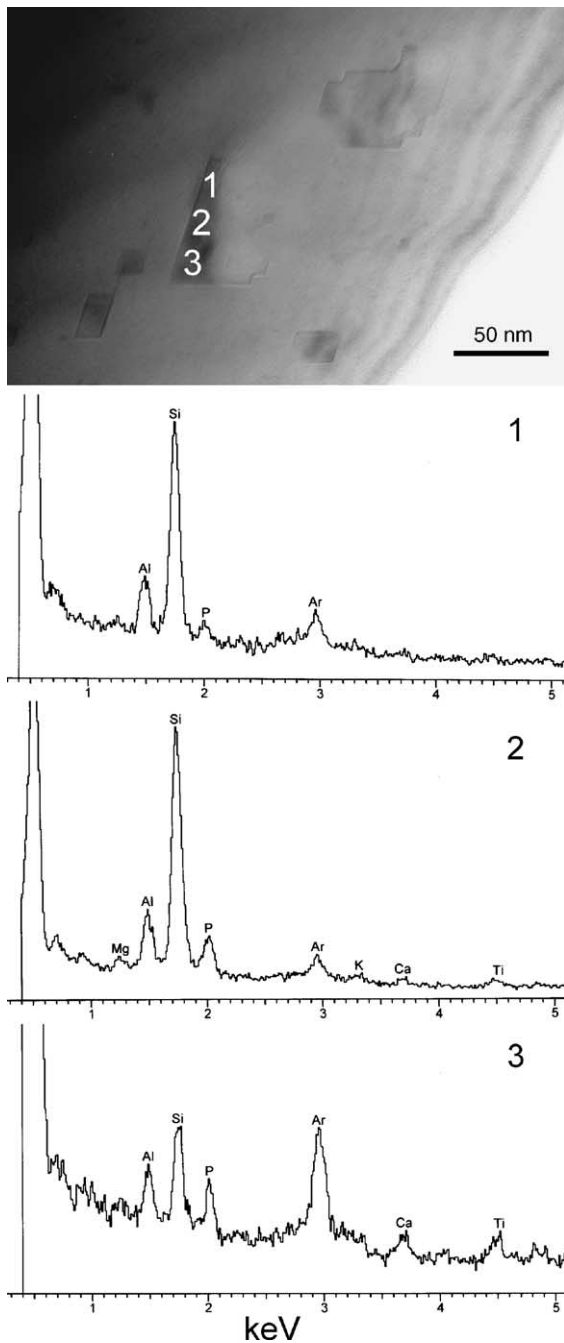
Fig. 4. AEM bright field image and associated EDX spectra showing the spatial compositional variation of the glass phase in an opened inclusion in diamond from gneiss of Kokchetav. The abscissa is X-ray energy in the unit of keV and the ordinate is X-ray intensity.

in garnet were observed once in KD301 (inset in Fig. 2d) [10]. Due to the limited observations and poor imaging condition, it was uncertain whether the pocket contains a fluid or a glass. The fluid/melt in the pocket is K-rich and Si-poor (see KD301 in Table 1), and is

presumably less viscous than the silicate melt in microdiamonds within garnet from the gneiss samples mentioned above.

4. Discussion

4.1. Rock-buffered formation media for metamorphic microdiamond

The newly discovered fluid/glass inclusions in metamorphic microdiamonds presented here, as well as those reported by Hwang et al. [10], clearly demonstrate that most metamorphic microdiamonds were formed through a fluid and/or a melt medium. The chemical characteristics of these media differ significantly and the different types of media seem to be related to the diverse types of host-rocks. Whereas, on a volatile-free basis, the ultrapotassic fluid medium found in microdiamonds within garnet from marble is SiO_2-poor, the glass (former melt) in microdiamonds within garnet from gneissic rocks is SiO_2-rich (Tables 1). Although the fluid/glass status of the intergranular pockets within microdiamond aggregates in garnet–quartz–clinopyroxene rocks cannot be ascertained as mentioned above, its chemical characteristics, however, seem to be in between those of melt and fluid media (see KD301 in Table 1). Chemical compositions of various host-rocks have been described by Shatsky et al. [21] and Massonne [22]. In essence, the gneisses are high in SiO_2 and the dolomite marbles are high in MgO and CaO, but low in SiO_2. On the other hand, the garnet–quartz–clinopyroxene rocks have compositions in between. The microdiamond formation media therefore have chemical characteristics mimicking their host

Table 2
Characteristics of metamorphic microdiamond and its inclusions in various rock types

Rock type	Gneiss	Grt–qtz–cpx rock	Dolomite marble
Diamond size	3–20 μm	3–10 μm	5–35 μm
Diamond morphology	cubo-octahedra, octahedral	cubo-octahedra, octahedral	Spheroid, cuboid
Inclusion type	glass	not clear	fluid
Inclusion number	moderate to abundant	none	abundant
Inclusion size	<30 nm	–	<500 nm
Phase separation in inclusion during e-beam heating	no	not clear	yes
Chemical characteristics of inclusion	high in Si, P, K	intermediate (intradiamond pockets)	high in K, low in Si

rocks, indicating that the former must have been compositionally buffered by the latter through melt/fluid-mineral elemental partition relations.

Since the respective fluids/melts with their distinct chemical characteristics mimicking the host-rocks are suggested to represent the microdiamond formation media in different host rocks, a straightforward postulation for the origin of these microdiamond formation media is that they were formed within the respective host-rocks through dehydration/decarbonation and/or partial melting processes, although the possibility of an external source also may exist. Thus, the derived fluid/melt was chemically buffered by the host-rock and (preferentially) extracted carbon from the respective host-rock. Consequently, it was able to become supersaturated with respect to carbon and to precipitate microdiamonds within the diamond stability field. Under such a scenario, the high K content of the fluid inclusions in microdiamonds from dolomite marble (Table 1) becomes somewhat puzzling, since that dolomite marble has a comparable but lower K content than gneisses (i.e., $\sim 1\%$ vs. $\sim 1-4\%$) [21]. In addition, microdiamonds from Kokchetav marble exhibit $\delta^{13}C$ values ranging from $-26.9‰$ to $-8.3‰$ [23], whereas diamond-bearing hosting marble is higher in $\delta^{13}C$ values, mostly (more than 80 analyses) in the range from $-7.0‰$ to $-1.0‰$, with one outlier at $-9.0‰$ [24]. Decomposition of K-bearing phases such as phlogopite in the dolomite marble system (e.g. [25]), involvement of ^{13}C-depleted organic carbon, continuous decarbonation process [26], heterogeneous isotopic compositions of dolomite, as well as loss of primary C-isotope signature of dolomite during exhumation [24], might have to be invoked to account for the observed geochemical features.

An alternative explanation is that the fluid medium in marble may in fact be derived from the melt medium resulted from partial melting of country rock gneiss if the melt (from outside) infiltrated into and reacted with the marble as was postulated by Hwang et al. [10]. The melt may thus loose its Si component through reaction with carbonates causing K enrichment in the more diluted reaction residue. The volatile content, such as CO_2, may increase during the infiltration leading toward a more fluid (than melt) nature of the medium following the general reaction: dolomitic marble + Si/Al in melt = silicates + CO_2.

In such a case, the C-isotope compositions of microdiamonds within garnet from dolomite marble would indicate that both crustal carbonaceous material in gneiss/marble and carbonate carbon in marble might have been involved in diamond genesis in addition to

the infiltration–decarbonation processes. In this regard, crustal carbonaceous material in gneissic rocks extracted through a partial melting process might be the major carbon source of microdiamonds in UHP gneissic rocks as was demonstrated by the very low C-isotope compositions of microdiamonds ($\sim -28‰$) in Erzgebirge gneiss [27].

One distinct feature of the glass inclusions within microdiamonds is their high P content (up to 30% P_2O_5; Table 1), despite the very low P content of the various host rocks (< 0.5%) [21,22] in these UHP terranes. Some phosphorous minerals, such as apatite, must have decomposed during the melt genesis. The high K content in these inclusions (up to 25% K_2O; Table 1) may also bear the same implication. It is also important to note that the possibility that partial melting of gneissic rocks was actually triggered by infiltration of an external K-rich fluid could not be excluded either. Further experimental work may shed light on the different types of fluids/melts generated from their respective host rocks and thus on the formation of diamond (e.g. [28]). It should also be noted that, despite the gross similarity, the composition of the glass inclusions within Erzgebirge microdiamonds differs in some respects from the melt composition integrated from the associated silicates in the diamond-bearing multiphase pockets within garnet postulated by Hwang et al. [6]. The latter is low in K_2O (3%) and P_2O_5 (2%) compared to the measured amounts of 5–18% K_2O and 11–31% P_2O_5 of the glass inclusions within microdiamonds in the present study. In addition to potential analytical uncertainties, the differences may be a result of crystallization fractionation. Alternatively, two media may develop at different stages of partial melting and/or infiltration.

If the microdiamonds were indeed crystallized from the melt/fluid media, the process would have most probably taken place during the exhumation stage, i.e., when T and P dropped and carbon became supersaturated within the media. This is consistent with the observation that microdiamond inclusions were mainly distributed at the margin of garnet core in gneissic rocks from both the Kokchetav and the Erzgebirge massifs [22]. The present data, however, cannot ascertain whether the melt/fluid media were formed during the prograde, the peak or the initial exhumation stage. Massonne [2] described the possible partial melting processes in UHP gneissic rocks and suggested that the irregular shape of garnet cores in these gneissic rocks in these two terranes may result from resorption reactions with partial melt at peak temperatures. It should be noted that partial melting of UHP gneissic rocks in the Kokchetav and the Erzgebirge massif has been inferred

from chemical compositions of gneisses, multiple-phase inclusions within garnet and petrographic observations [21,22]. The identification of glass inclusions in microdiamonds within garnet in the present study provides a piece of direct evidence supporting the previous postulation. The presence of a melt phase in UHP rocks bears important implications for rock rheology as well as mechanism of rock exhumation, although the amount of melt present and the possible glass transition remain to be studied.

"Fluid" inclusions are also common in cuboid kimberlitic diamonds, and in the fibrous coats of coated kimberlitic diamonds, but are rare in octahedral kimberlitic diamonds [28]. Chemical analyses of these inclusions within kimberlitic diamonds indicate three end members: a carbonatitic melt, a hydrous-silicic melt rich in water, Si, Al and K, and a brine rich-in Cl, K and Na [29–32]. Compared to these compositions, the fluid/glass inclusions in metamorphic microdiamonds are significantly enriched in Si+Al and K but low in Cl and Ca+Mg+Fe+Na (Fig. 5). In terms of the amounts of Si+Al, K and Ca+Mg+Fe+Na, the host-rock buffering effect, i.e., mantle rocks vs. crustal rocks, may in part explain the difference. The brine end-member, important for kimberlitic diamonds, might not be important for the formation of metamorphic microdiamond, although a trapped brine solution was suggested in metamorphic microdiamond in Kokchetav garnet–clinopyroxene rocks [33]. Based on the chemical variations of fluid inclusions within kimberlitic diamonds, Klein-BenDavid et al. [32] claimed that the carbonatitic melt might evolve to the hydrous-silicic and brine end members and be the ultimate source medium of kimberlitic diamond formation. Since a SiO$_2$-poor fluid medium might evolve from a SiO$_2$-rich melt through infiltration into the dolomite marble, as mentioned above, the host-rock buffering effect plays a decisive role for any fluid/melt for the formation of microdiamonds in UHP metamorphic rocks.

4.2. Microdiamond morphology mediated by the nature of the formation medium

Each diamond-bearing rock type of the Kokchetav massif contains microdiamonds with a distinctive range of morphologies according to OM and/or scanning electron microscopy [34–36]. For example, microdiamonds occurring within garnet in marbles and garnet–clinopyroxene rocks are predominantly cuboid in shape. Biotite gneisses are characterized by containing a cubo-octahedral microdiamond population, although a few cuboids and skeletals also exist [34–37]. Octahedral
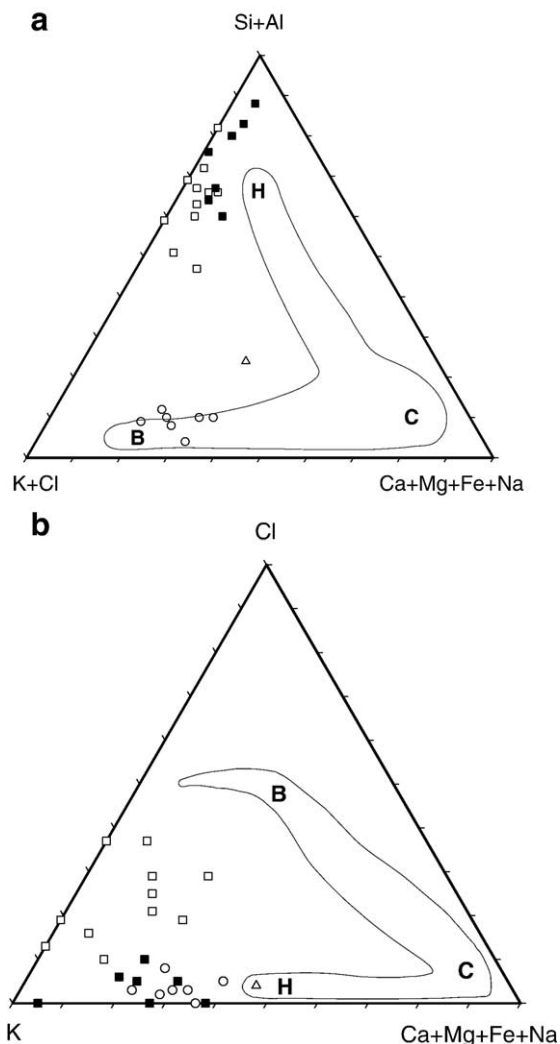

Fig. 5. Compositional variations of glass inclusions in microdiamonds in (a) Si+Al–K+Cl–Ca+Mg+Fe+Na and (b) Cl–K–Ca+Mg+Fe+Na projections after Klein-BenDavid et al. [33]. Solid line shows the composition field of fluid inclusions in mantle diamond; H denotes the hydrous-silicic melt endmember, C represents the carbonatitic melt endmember, and B is the brine-rich endmember defined in [33]. Solid squares: glass inclusions in Erzgebirge gneiss; open squares: glass inclusions in Kokchetav gneiss; open circles: fluid inclusions in Kokchetav marble; and open triangle: glass–fluid inclusions in Kokchetav garnet–quartz–clinopyroxene rock. The compositions of the latter two are taken from Hwang et al. [10].

microdiamonds are only observed in zoisite gneiss [38]. The present AEM studies of microdiamond inclusions in garnets show that, with exceptions, a rough generalization can be established between microdiamond morphology and host rock types. Microdiamond inclusions within garnet from gneissic samples and garnet–quartz–clinopyroxene rocks are largely bounded by {111} and {100} faces. On the other hand, microdiamonds within

garnet from dolomite marble are usually cuboid/spheroid in shape with fibrous internal structures and very rugged surfaces. These AEM observations are in general consistent with previous studies [34–36].

It has been suggested that the morphologies of diamonds are mostly dictated by their growth kinetics (e.g. [20]). Higher temperatures or lower degrees of carbon supersaturation in the formation media favor octahedron, whereas lower temperatures or higher degrees of carbon supersaturation results in cuboid shapes. However, the variation of other "conditions" of the formation medium is surely also important. For example, increasing water and/or Mg content may favor skeletal morphology, whereas carbonate melt tends to form octahedron [20,39,40].

It may not be reasonable to assume that the microdiamonds studied here were all formed at similar temperatures. However, the peak metamorphic temperatures of the Erzgebirge and the Kokchetav massifs are high and tolerably similar, i.e., about 1200 °C and 950–1100 °C, respectively [22,41]. The temperature factor may thus be considered not too critical in affecting the growth kinetics of microdiamonds, and the chemical characteristics of the fluid/melt may be the controlling factor for variations of morphology, especially for microdiamonds with different morphologies in various rock types as described for the Kokchetav massif. It therefore seems likely that the P/K-rich silica melt favors octahedral or cubo-octahedral forms, whereas the SiO_2-poor ultrapotassic fluid tends to form spheroids/cuboids. Note that the fluid inclusions in metamorphic microdiamonds are usually abundant and larger in size (i.e. <500 nm), but the glass inclusions are mostly smaller in size (i.e. <30 nm) (Table 2). This, along with the much larger crystal sizes and the more rugged surfaces of microdiamonds within garnet from marble, clearly demonstrates that the microdiamond growth rate/growth mechanism in marble is faster than/different from that in gneissic rocks or garnet–quartz–clinopyroxene rocks. However, whether such a difference was due to different degrees of carbon supersaturation, different K and/or Ca content, or different viscosity of the formation media remains to be studied.

5. Conclusions

Abundant nanometer-size facetted P/K-rich silica glass (former melt) inclusions were identified in microdiamonds from garnets of the Kokchetav and the Erzgebirge UHP gneisses. These findings demonstrate that, besides the ultrapotassic COH fluids for the genesis of microdiamonds in marble [10], metamorphic micro-

diamonds could also form from P/K-rich silica melts. These glass inclusions are characteristically smaller in size and higher in Si/lower in K than the fluid inclusions [10]. All these fluid/glass inclusions actually show chemical characteristics mimicking their host-rocks, suggesting that the microdiamond formation media might have been generated within their respective host-rocks through partial melting of gneissic rocks and/or dehydration/decarbonation processes in marble. Alternatively, melt from gneisses may also be able to infiltrate into and react with the dolomite marble, changing its chemical compositions and evolving from melt toward a "more" fluid status. In either case, the respective fluid/melt medium was obviously compositionally buffered by its respective host-rock through fluid/melt-mineral elemental partition relations. Crustal carbonaceous material may be the major carbon source of microdiamonds in UHP gneissic rocks, whereas carbon derived from carbonates may also play an additional role for microdiamond formation, especially in UHP dolomite marble. Chemical differences between the formation media of the metamorphic diamond and mantle diamond are also demonstrated. The former is higher in Si+Al and K but lower in Cl and Ca+Mg+Fe+Na compared with the latter. Some of these differences can be partly attributed to the host-rock buffering effect introduced here. Since the fluid/melt media for metamorphic microdiamond genesis must have been buffered by the hosting rocks, it might not be possible to deduce the primary compositions/characteristics of the medium by its major chemical compositions, if the medium has an external origin.

The morphology of the metamorphic microdiamonds in different host rocks varies. If the temperature effect can be considered to be minimal, the different morphologies of these metamorphic microdiamonds may most likely be related to the respective different nature of the formation medium. The P/K-rich silica melt medium favors an octahedral or cubo-octahedral form, whereas the K-rich fluid medium tends to take on a cuboid or spheroid form with rugged surfaces. The diamond growth rate/mechanism in the fluid medium is thus different from that in the melt medium. In order to detect the governing factor causing this difference, however, more detailed and primarily also experimental studies remain to be done.

References

[1] N.V. Sobolev, V.S. Shatsky, Diamond inclusions in garnets from metamorphic rocks, a new environment for diamond formation, Nature 343 (1990) 742–746.

[2] H.J. Massonne, A new occurrence of microdiamonds in Quartzofeldspathic rocks of the Saxonian Erzgebirge, Germany, and their metamorphic Evolution, in: J.J. Gurney, J.L. Gurney, M.D. Pascoe, S.H. Richardson (Eds.), Proceedings of the 7th International Kimberlite Conference, vol. 2, Red Roof Design cc, Cape Town, South Africa, 1999, pp. 533–539.

[3] J. Yang, Z. Su, L.F. Dobrzhinetskaya, H.W. Green, X. Pei, R. Shi, C. Wu, J.L. Wooden, J. Zhang, Y. Wan, H. Li, Discovery of metamorphic diamonds in central China: an indication of a >4000-km-long zone of deep subduction resulting from multiple continental collisions, Terra Nova 15 (2003) 370–379.

[4] I. Katayama, A. Zayachkovsky, S. Maruyama, Prograde pressure–temperature records from inclusions in zircons from ultrahigh-pressure rocks of the Kokchetav massif, northern Kazakhstan, Isl. Arc 9 (2000) 417–427.

[5] K. De Corte, P. Cartigny, V.S. Shatsky, N.V. Sobolev, M. Javoy, Evidence of fluid inclusions in metamorphic microdiamonds from the Kokchetav massif, northern Kazakhstan, Geochim. Cosmochim. Acta 62 (1998) 3765–3773.

[6] S.L. Hwang, P. Shen, H.T. Chu, T.F. Yui, C.C. Lin, Genesis of microdiamonds from melt and associated multiphase inclusions in garnet of ultrahigh-pressure genesis from Erzgebirge, Germany, Earth Planet. Sci. Lett. 188 (2001) 9–15.

[7] B. Stöckhert, J. Duyster, C. Trepmann, H.J. Massonne, Microdiamond daughter crystals precipitated from supercritical COH+ silicate fluids included in garnet, Erzgebirge, Germany, Geology 29 (2001) 391–394.

[8] L.F. Dobrzhinetskaya, H.W. Green, K.N. Bozhilov, T.E. Mitchell, R.M. Dickerson, Crystallization environment of Kazakhstan microdiamond: evidence from nanometric inclusions and mineral associations, J. Metamorph. Geol. 21 (2003) 425–437.

[9] H. Bureau, H. Keppler, Complete miscibility between silicate melts and hydrous fluids in the upper mantle: experimental evidence and geochemical implications, Earth Planet. Sci. Lett. 165 (1999) 187–196.

[10] S.L. Hwang, P. Shen, H.T. Chu, T.F. Yui, J.G. Liou, N.V. Sobolev, V.S. Shatsky, Crust-derived potassic fluid in metamorphic microdiamond, Earth Planet. Sci. Lett. 231 (2005) 295–306.

[11] S.L. Hwang, P. Shen, T.F. Yui, H.T. Chu, Metal–sulfur–COH–silicate fluid mediated diamond nucleation in Kokchetav ultrahigh-pressure gneiss, Eur. J. Mineral. 15 (2003) 503–511.

[12] V.S. Shatsky, N.V. Sobolev, The Kokchetav massif of Kazakhstan, in: D.A. Carswell, R. Compagnoni (Eds.), Ultrahigh Pressure Metamorphism, Eötvös University Press, Budapest, 2003, pp. 75–103.

[13] H.J. Massonne, P. O'Brien, The Bohemian massif and the NW Himalaya, in: D.A. Carswell, R. Compagnoni (Eds.), Ultrahigh Pressure Metamorphism, Eötvös University Press, Budapest, 2003, pp. 145–187.

[14] N.V. Sobolev, V.S. Shatsky, J.G. Liou, R.Y. Zhang, S.L. Hwang, P. Shen, H.T. Chu, T.F. Yui, A.A. Zayachkovsky, M.A. Kasymov, US–Russian Civilian Research and Development Fund Project: an origin of microdiamonds in metamorphic rocks of the Kokchetav massif, northern Kazakhstan, Episodes 26 (2003) 290–294.

[15] O. Navon, Chemical and mineralogy characterization of micro-inclusions in diamonds, Ph.D. Dissertation, California Inst. Technol. (1989).

[16] M.H. Loretto, Electron Beam Analysis of Materials, Chapman & Hall, London, 1994, pp. 197–214.

[17] M.R. Carroll, J.D. Webster, Solubilities of sulfur, noble gases, nitrogen, chlorine, and fluorine in magmas, Rev. Miner. 30 (1994) 231–279.

[18] B.O. Mysen, M. Acton, Water in H_2O-saturated magma–fluid systems: solubility behavior in $K_2O–Al_2O_3–SiO_2–H_2O$ to 2.0 GPa and 1300 °C, Geochim. Cosmochim. Acta 63 (1999) 3799–3815.

[19] L.F. Dobrzhinetskaya, H.W. Green, M. Weschler, M. Darus, Y.C. Wang, H.J. Massonne, B. Stöckhert, Focused ion beam technique and transmission electron microscope studies of microdiamonds from the Saxonian Erzgebirge, Germany, Earth Planet. Sci. Lett. 210 (2003) 399–410.

[20] I. Sunagawa, Growth and morphology of diamond crystals under stable and metastable conditions, J. Cryst. Growth 99 (1990) 1156–1161.

[21] V.S. Shatsky, E. Jagoutz, N.V. Sobolev, O.A. Kozmenko, V.S. Parkhomenko, M. Troesch, Geochemistry and age of ultrahigh pressure metamorphic rocks from the Kokchetav massif (Northern Kazakhstan), Contrib. Mineral. Petrol. 137 (1999) 185–205.

[22] H.J. Massonne, A comparison of evolution of diamondiferous quartz-rich rocks from the Saxonian Erzgebirge and the Kokchetav Massif: are so-called diamondiferous gneisses magmatic rocks? Earth Planet. Sci. Lett. 216 (2003) 347–364.

[23] K. Imamura, Y. Ogasawara, H. Yurimoto, M. Kusakabe, Carbon isotope compositions of microdiamond in UHP marble, Abstracts of 32nd International Geological Congress, Florence, Italy, Part 1, 2004, pp. 720–721.

[24] M. Ohta, T. Mock, Y. Ogasawara, D. Rumble, Oxygen, carbon, and strontium isotope geochemistry of diamond-bearing carbonate rocks from Kumdy-Kol, Kokchetav Massif, Kazakhstan, Lithos 70 (2003) 77–90.

[25] Y. Tatsumi, Migration of fluid phases and genesis of basalt magmas in subduction zones, J. Geophys. Res. 94 (1989) 4697–4707.

[26] P. Cartigny, J.W. Harris, M. Javoy, Eclogitic diamond formation at Jwaneng: no room for a recycled component, Science 280 (1998) 1421–1424.

[27] H.J. Massonne, Genesis of diamonds and diamondiferous rocks from the Saxonian Erzgebirge, Central Europe, 7th International Eclogite Conference, Seggau, Austria, Mitt. Osterr. Mineral. Ges., vol. 150, 2005, p. 104.

[28] J.W. Harris, Diamond geology, in: J.E. Field (Ed.), The Properties of Natural and Synthetic Diamonds, Academic Press, London, 1992, pp. 345–393.

[29] O. Navon, I.D. Hutcheon, G.R. Rossman, G.J. Wasserburg, Mantle-derived fluids in diamond micro-inclusions, Nature 335 (1988) 784–789.

[30] M. Schrauder, O. Navon, Hydrous and carbonatitic mantle fluids in fibrous diamonds from Jwaneng, Botswana, Geochim. Cosmochim. Acta 58 (1994) 761–771.

[31] E.S. Izraeli, J.W. Harris, O. Navon, Brine inclusions in diamonds: a new upper mantle fluid, Earth Planet. Sci. Lett. 187 (2001) 323–332.

[32] O. Klein-BenDavid, E.S. Izraeli, E. Hauri, O. Navon, Mantle fluid evolution—a tale of one diamond, Lithos 77 (2004) 243–253.

[33] K. De Corte, P. Cartigny, V.S. Shatsky, P. De Paepe, N.V. Sobolev, M. Javoy, Characteristics of microdiamonds from UHPM rocks of the Kokchetav Massif (Kazakhstan), in: J.J. Gurney, L.G. Gurney, M.D. Pascoe, S.H. Richardson (Eds.), Proceedings of the 7th International Kimberlite Conference, vol. 1, Red Roof Design cc, Cape Town, South Africa, 1999, pp. 174–182.

[34] K. De Corte, W.R. Taylor, P. De Paepe, Inclusion contents of microdiamonds from UHP metamorphic rocks of the Kokchetav massif, in: C.D. Parkinson, I. Katayama, J.G. Liou, S. Maruyama (Eds.), The Diamond-Bearing Kokchetav Massif, Kazakhstan, Universal Academy Press Inc., Tokyo, 2002, pp. 115–135.

[35] V.S. Shatsky, G.M. Rylov, E.S. Efimova, K. De Corte, N.V. Sobolev, Morphology and real structure of microdiamonds from metamorphic rocks of the Kokchetav Massif, kimberlites, and alluvial placers, Russ. Geol. Geophys. 39 (1998) 949–961.

[36] V.S. Shatsky, K. De Corte, N.V. Sobolev, Microdiamonds, in: N.L. Dobrestov, N.V. Sobolev, V.S. Shatsky (Eds.), Field Guide Book, Diamondiferous and High-Pressure Metamorphic Rocks of the Kokchetav Massif (Northern Kazakhstan), Fourth International Eclogite Field Conference, Novosibirsk, 1999, pp. 37–63.

[37] A.V. Korsakov, V.S. Shatsky, N.V. Sobolev, A.A. Zayachokovsky, Garnet–biotite–clinozoisite gneiss: a new type of diamondiferous metamorphic rock from the Kokchetav Massif, Eur. J. Mineral. 14 (2002) 915–928.

[38] L.F. Dobrzhinetskaya, H.W. Green II, T.E. Mitchell, R.M. Dickerson, Metamorphic diamonds: mechanism of growth and inclusion of oxides, Geology 29 (2001) 263–266.

[39] Y.N. Pal'yanov, A.G. Sokol, Y.M. Borzdov, A.F. Khokhryakov, N.V. Sobolev, Diamond formation from mantle carbonate fluids, Nature 400 (1999) 417–418.

[40] L.F. Dobrzhinetskaya, A.P. Renfro, H.W. Green, Synthesis of skeletal diamonds: implications for microdiamond formation in orogenic belts, Geology 32 (2004) 869–872.

[41] C.D. Parkinson, S. Maruyama, J.G. Liou, M.J. Kohn, Probable prevalence of coesite-stable metamorphism in collisional orogens and a reinterpretation of Barrovian metamorphism, in: C.D. Parkinson, I. Katayama, J.G. Liou, S. Maruyama (Eds.), The Diamond-Bearing Kokchetav Massif, Kazakhstan, Universal Academy Press Inc., Tokyo, 2002, pp. 447–461.